Clin Physiol Funct Imaging (2014) **34**, pp163–170 doi: 10.1111/cpf.12083

INVITED REVIEW

Review: comparison of PET rubidium-82 with conventional SPECT myocardial perfusion imaging

Adam A. Ghotbi, Andreas Kjær and Philip Hasbak

Department of Clinical Physiology, Nuclear Medicine & PET and Cluster for Molecular Imaging, Rigshospitalet, University of Copenhagen, Copenhagen, Denmark

Summary

Nuclear cardiology has for many years been focused on gamma camera technology. With ever improving cameras and software applications, this modality has developed into an important assessment tool for ischaemic heart disease. However, the development of new perfusion tracers has been scarce. While cardiac positron emission tomography (PET) so far largely has been limited to centres with on-site cyclotron, recent developments with generator produced perfusion tracers such as rubidium-82, as well as an increasing number of PET scanners installed, may enable a larger patient flow that may supersede that of gamma camera myocardial perfusion imaging.

Correspondence
Adam A. Ghotbi, Rigshospitalet, Copenhagen University Hospital, Blegdamsvej 9, 2100 Copenhagen, Denmark
E-mail: adamghotbi@gmail.com

Accepted for publication
Received 11 April 2013; accepted 14 August 2013

Key words
cardiac PET; cardiac SPECT; cardiology; myocardial perfusion imaging; rubidium

Introduction

Myocardial perfusion imaging (MPI) has been a cornerstone in the assessment of patients with known or suspected coronary artery disease (CAD). Single photon emission computed tomography (SPECT) is a well-established modality for the diagnosis and risk stratification of patients suspected for ischaemic heart disease (Navare *et al.*, 2004). In the mid-1970s, the discovery of thallium-201 (^{201}TI) made it possible to provide information on myocardial perfusion, objectively and non-invasively (Zaret & Cohen, 1977). ^{201}TI, being a relatively good perfusion tracer, is not optimal for clinical cardiac imaging due to high radiation burden and low energy emission with poorer image quality. With the introduction of technetium-99m (^{99m}Tc) labelled perfusion tracers (^{99m}Tc-sestabimi and ^{99m}Tc-tetrofosmine), there were now clear alternatives to ^{201}Tl. ^{99m}Tc, with a photo peak of 140 keV, has optimal energy for gamma camera detection. The half-life of 6 h enables administration of higher activity and results in better count statistics and picture quality with enhanced signal-to-noise ratio compared with ^{201}Tl. The continuous development in cardiac software applications has facilitated the measurements of wall thickening, left ventricle ejection fraction (LVEF) and wall movement of the left ventricle.

With positron emission tomography (PET) scanners being installed in large numbers in North America, Japan and Europe in recent years, primarily driven by the high demand for 18F-fluorodeoxyglucose (^{18}F-FDG) PET imaging in oncology, more and more departments can offer cardiac PET. Thus, with readily available tracers, PET is now regarded a usable alternative to conventional cardiac SPECT with rubidium-82 (^{82}Rb) becoming the most widely used radionuclide for the assessment of myocardial perfusion with PET.

The classical myocardial scintigraphy

In Europe, the ^{99m}Tc-based tracers are most commonly used for cardiac SPECT. ^{99m}Tc is extracted from blood circulation and accumulated in mitochondria of the myocyte. Image acquisition is obtained by rotating detectors, constituting SPECT. The prognostic and diagnostic values of cardiac SPECT in patients with ischaemic heart disease are well established (Hesse *et al.*, 2008; Marcassa *et al.*, 2008). Recently cardiac SPECT was highlighted in European Society of Cardiology Guidelines on myocardial revascularization with class 1A recommendation for use in patients with intermediate pretest likelihood of obstructive coronary disease (Wijns *et al.*, 2010).

Subjects performing exercise cardiac SPECT with a normal results – with the exception of patients with diabetes or chronic renal failure – have a very good prognosis and a one-year risk for death or non-fatal myocardial infarct of <1%, while patients with an abnormal test results have a corresponding risk of 6% (Shaw & Iskandrian, 2004; Venkataraman *et al.*, 2008). However, patients undergoing a pharmacological stress test are at a higher risk for subsequent cardiac events, regardless of a normal perfusion imaging result, compared

34, 3, 163–170

with subject performing exercise cardiac SPECT (Navare *et al.*, 2004).

The ability of cardiac SPECT to examine ischaemia, viability and left ventricle function makes it a well-validated, valuable and cost-effective clinical tool for the evaluation of ischaemic heart disease (Klocke *et al.*, 2003; Hachamovitch *et al.*, 2004).

However, SPECT displays a number of disadvantages compared with PET. Non-uniform attenuation artefacts and the low heart-to-background ratio of SPECT reduce the specificity to detect coronary artery disease (Tamaki *et al.*, 1988; Rigo *et al.*, 1998; Aarnoudse *et al.*, 2003). However, the use of transmission scan with CT or radioactive sources has improved diagnostic accuracy (Kjaer *et al.*, 2002). Furthermore, cardiac SPECT permits only semi-quantitative measurements of changes in regional perfusion, and in the case of subjects with balanced ischaemia (i.e. three vessel disease, microvascular disease) or submaximal hyperaemia due to intake of methylxanthine containing food or beverages (i.e. coffee) prior to pharmacologic stress with dipyridamole, adenosine or regadenosone, a false-negative result is likely due to homogenous tracer uptake (Ito *et al.*, 2003; Lima *et al.*, 2003; Storto *et al.*, 2009).

Positron emission tomography

The radionuclide tracers utilized in PET all decay by emission of positrons. The positron is emitted from the nucleus and rapidly looses kinetic energy before colliding with an electron. Both particles annihilate and emit 2 gamma rays with energies of 511 keV. The two gamma rays travel in opposite directions with a relative angel very close to 180 degrees. Thus, if the ring of detectors surrounding the patient in a PET scanner detects a coincidence pair of 511 keV gamma rays, it is registered as an event. When many such events are detected, the activity distribution of the positron-emitting radionuclide within the volume of interest (e.g. the left ventricle) may be constructed. Cardiac PET provides better spatial resolution and sensitivity compared with cardiac SPECT and has the ability of robust attenuation correction. Reliable attenuation correction methods for PET require determination of an attenuation map, which represents the spatial distribution of linear attenuation coefficients at 511 keV.

After the attenuation map is generated, it can be incorporated into image reconstruction algorithms to correct the emission data for errors contributed by photon attenuation. Attenuation maps are usually generated by transmission scanning using external radionuclide sources or in recent years with the availability of PET/CT scanners based on X-rays.

PET has a higher sensitivity than SPECT. SPECT is limited by collimation, whereas PET is limited by high photon energy. A typical detection efficiency for a collimated SPECT detector is in the order of 0·01%, whereas modern three-dimensional (3D) PET scanners have detection efficiencies around 0·5% or higher (Di Carli, 2007; Rahmim & Zaidi, 2008).

The most common perfusion tracers for clinical cardiac PET are ^{13}N-labelled ammonia ($^{13}NH_3$), ^{82}Rb and ^{15}O-labelled water ($H_2{}^{15}O$; Schelbert *et al.*, 1982; Selwyn *et al.*, 1982; Walsh *et al.*, 1988). $^{13}NH_3$ and $H_2{}^{15}O$ production needs a cyclotron, thereby limiting the availability to larger centres with in-house cyclotrons, and the tracers are primarily used for research due to a laborious workflow.

^{82}Rb is a potassium analogue that is generator produced with a physical half-life of 75 s and kinetic properties similar to those of ^{201}Tl (Di Carli & Lipton 2007). Its parent radionuclide is strontium-82 (^{82}Sr), which has a physical half-life of 26 days. Consequently, the ^{82}Sr/^{82}Rb generator only needs to be replaced every 4–6 week. The short physical half-life of ^{82}Rb and the rapid reconstitution of the generator allow fast sequential perfusion imaging and high patient throughput.

After intravenous injection, ^{82}Rb rapidly crosses the capillary membrane. Myocardial uptake of ^{82}Rb requires active transport via the sodium/potassium adenosine triphosphate transporter, which is dependent on coronary blood flow (Selwyn *et al.*, 1982). The single-capillary transit extraction fraction of ^{82}Rb exceeds 50%. However, as other non-diffusible tracers, its net extraction fraction decreases in a nonlinear fashion with increasing myocardial blood flow (Selwyn *et al.*, 1982; Goldstein *et al.*, 1983; Mullani *et al.*, 1983). However, quantification of myocardial blood flow with ^{82}Rb was validated against $H_2{}^{15}O$ and found to be accurate at high flow rates (Prior *et al.*, 2012).

The maximum kinetic energy of positrons emitted during ^{82}Rb decay is significantly higher than that of ^{18}F or ^{13}N. Consequently, the spatial uncertainty in the location of the decaying nucleus – which depends on the distance travelled by the positrons before their annihilation (positron range) – is greater for ^{82}Rb (mean positron range 2·6 mm) than for ^{18}F (0·2 mm) or ^{13}N (0·7 mm; Di Carli, 2007). Although ^{82}Rb imaging yields excellent image quality with current PET technology, its longer positron range and its short half-life, which requires significant image smoothing to suppress noise, both mitigate somewhat the improved spatial resolution of PET.

As indicated earlier, cardiac SPECT possesses great qualities in diagnosis of ischaemic heart disease (IHD). Several studies report the sensitivity and specificity of cardiac SPECT for detecting an angiographically significant stenosis of >50% to be 87% [95% confidence interval (CI) 71–97%], and 73% (CI 36–100%), respectively (Klocke *et al.*, 2003). Corresponding sensitivity and specificity for cardiac perfusion PET are reported to be 91% (CI 83–100%) and 89% (CI 73–100%), respectively (Di Carli *et al.*, 2007b).

In a recent systematic review and meta-analysis evaluating the accuracy of ^{82}Rb PET for the diagnosis of obstructive coronary artery disease in comparison with cardiac SPECT, 15 ^{82}Rb- PET and eight cardiac SPECT studies were reviewed (Mc Ardle *et al.*, 2012). ^{82}Rb- PET demonstrated sensitivity and specificity of 90% and 88% for the detection of obstructive coronary disease on invasive coronary angiography (Fig. 1).

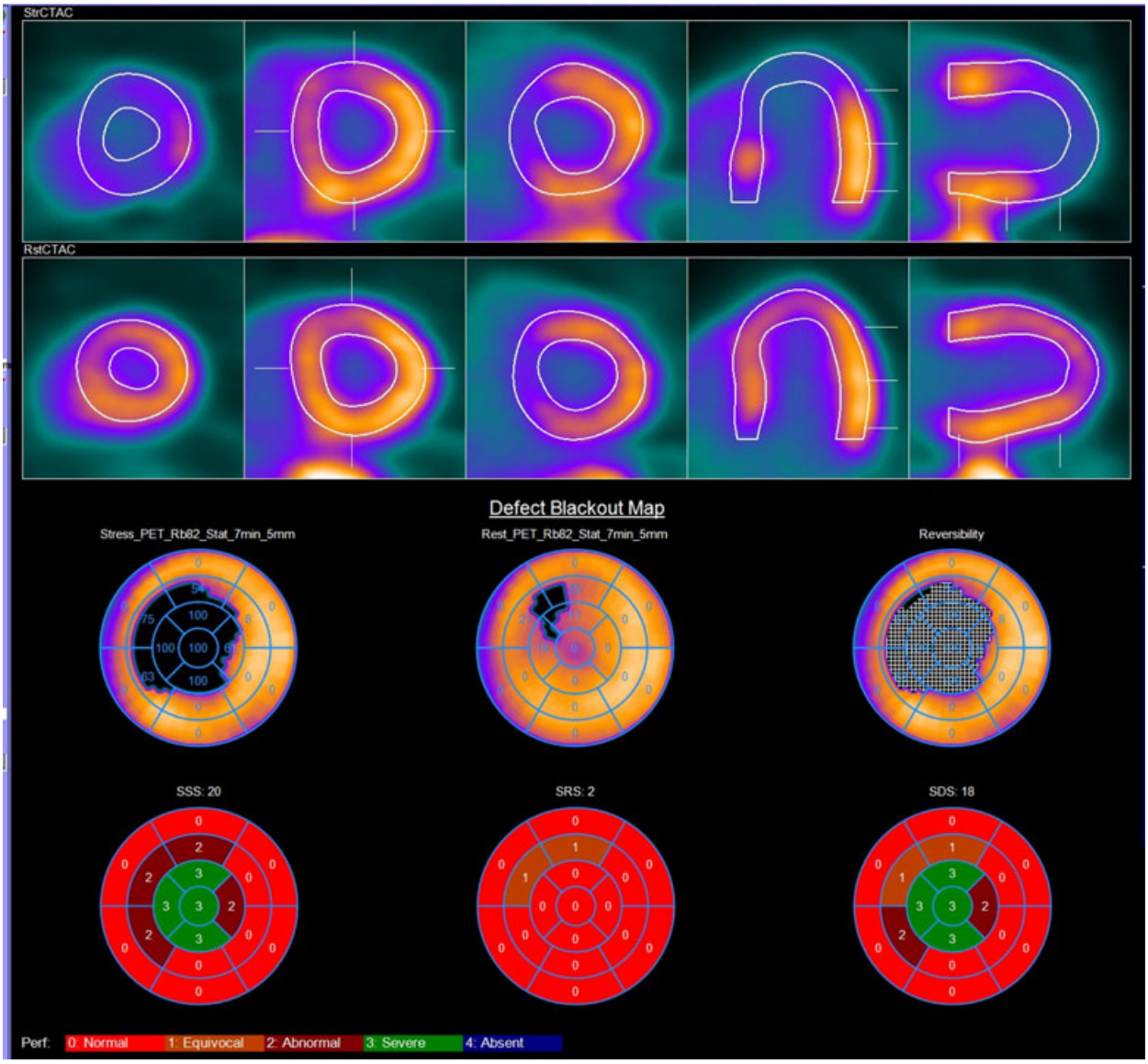

Figure 1 ^{82}Rb Cardiac PET; pharmacological stress test (adenosine) and rest test of a patient with suspected ischaemic heart disease. Significant decreased activity in stress test in LAD supply area, indicating reversible ischaemia. Patient was referred to invasive cardiac unit, resulting in stenting of a 95% narrowing of LAD. ^{82}Rb isotope administered during pharmacological stress and rest. Static recordings for 7 min in both phases. Upper row: pharmacological stress cardiac test. Lower row: rest test. Bulls Eye plots in 17 segments for both stress and rest test. LAD: Left anterior descending artery.

^{82}Rb- PET was demonstrated to have superior accuracy in comparison with ^{99m}Tc- SPECT with both ECG-gating and attenuation correction (Mc Ardle *et al.*, 2012).

PET quantification of myocardial blood flow is well validated using ^{13}N-ammonia (Kuhle *et al.*, 1992; Muzik *et al.*, 1993; Nitzsche *et al.*, 1996). Quantitative approaches with ^{82}Rb are more challenging because of its very short physical half-life and, thus, decreased image signal-to-noise ratio, leading to noisy and inconsistent time–activity curves that can affect the accuracy of myocardial perfusion estimates. However, the use of noise-reduction methods improves the accuracy and precision of measurements of myocardial blood flow (Lin *et al.*, 2001a,b). Validation studies of ^{82}Rb in humans have been performed and have shown high accordance with $^{13}NH_3$ perfusion values (El Fakhri *et al.*, 2009), the latter has previously been well validated with microspheres (Schelbert *et al.*, 1979).

Quantifying myocardial blood flow and the coronary flow reserve (CFR) have been determined by dynamic acquisition and tracer kinetic models (Parkash *et al.*, 2004; Di Carli *et al.*, 2007b).

PET has the capability to quantify flow in absolute terms (ml min^{-1} g^{-1}) during stress and rest, the ratio of which is also known as the coronary flow reserve (Fig. 2) (CFR; Camici & Crea, 2007; deKemp *et al.*, 2007). Measurement of CFR may have a role in early detection of coronary atherosclerotic

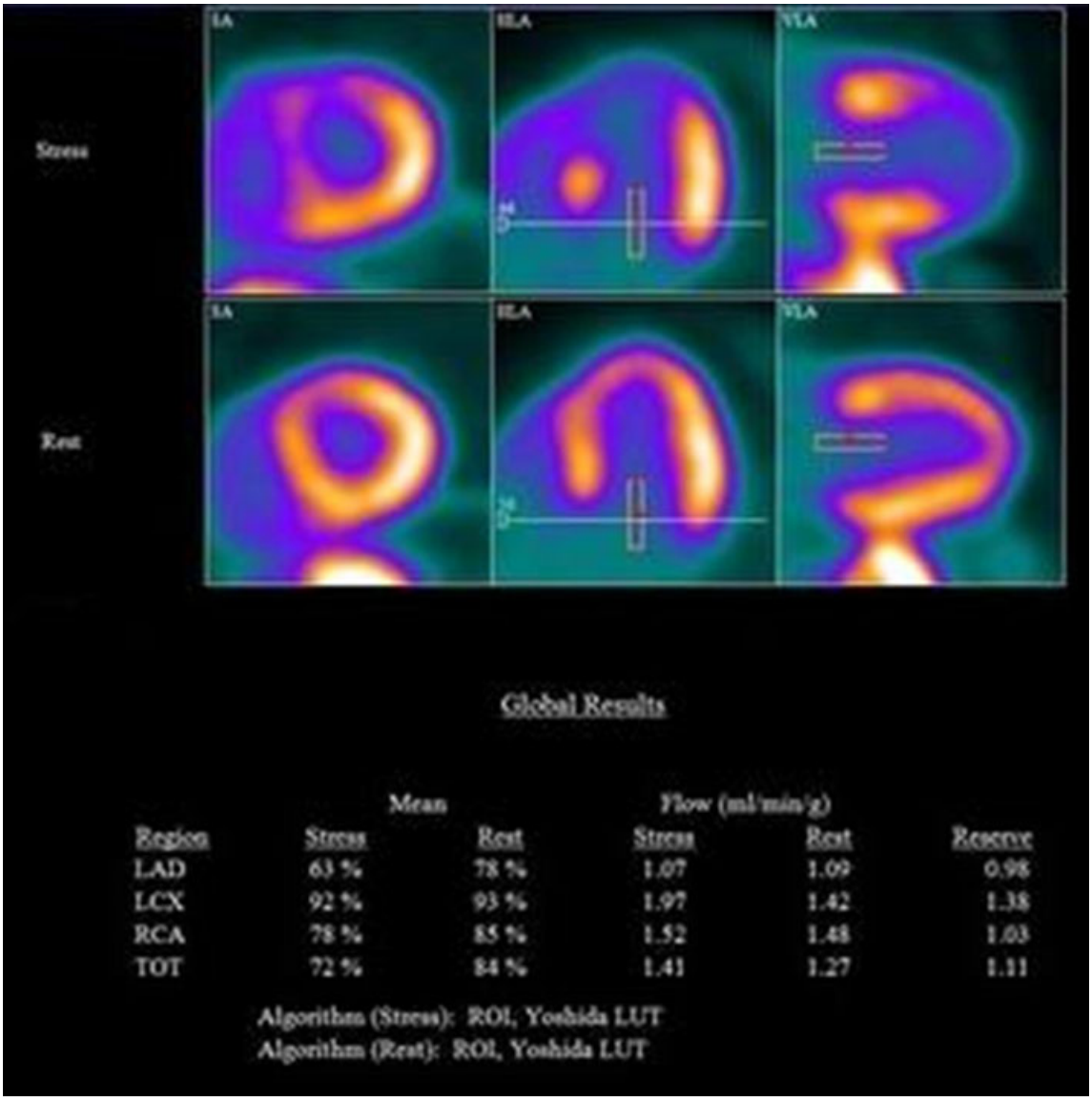

Figure 2 Quantifying blood flow with ^{82}Rb Cardiac PET (Yoshida *et al.*, 1996): pharmacological stress test (adenosine) and rest test of a patient with suspected ischaemic heart disease. Coronary flow reserve significantly decreased in LAD supply area. ^{82}Rb isotope administered during pharmacological stress and rest. Dynamic recordings for 7 min in both phases. Upper row: pharmacological stress cardiac test. Lower row: rest test. LAD, Left anterior descending artery; LCX, Left circumflex artery; RCA, Right coronary artery. Global: global flow in the left ventricle.

disease (microvascular dysfunction) or reveal the presence of diffuse (balanced) obstructive CAD (Parkash *et al.*, 2004; Camici & Crea, 2007). Although this approach has been firmly established in research settings almost three decades ago (Schelbert *et al.*, 1981), a widespread use in the clinical setting has still to be realized. Even so, there is growing interest in its potential added value due to the current limitations of relative MPI in these settings. Recently, one of the first studies to evaluate the prognostic value of PET-derived quantification of CFR using $^{13}NH_3$ in patients with suspected ischaemia and one of the first studies to evaluate its added prognostic value compared with relative MPI were published (Herzog *et al.*, 2009). The effect of CFR may be hampered when imaging with ^{82}Rb because of the nonlinearity between actual myocardial blood flow and k1 (measured flow). Nonetheless, in a recently published paper, impaired CFR was an independent risk in symptomatic patients with a normal PET MPI (Naya *et al.*, 2013). Confirming this in patients with known or suspected CAD, a multicenter observational study showed that the extent and severity of ischaemia and scar on PET MPI provided incremental risk estimates of cardiac death and all-cause death compared with traditional coronary risk factors (Dorbala *et al.*, 2013). Later several studies have shown the value in demonstrating subclinical abnormalities in myocardial blood flow or CFR in multiple patient cohorts including obese patients, diabetics, smokers, patients with hypertension and HIV-infected patients (Kaufmann *et al.*, 2000; Kjaer *et al.*, 2003, 2005; Schindler *et al.*, 2006, 2009; Kristoffersen *et al.*, 2010;

Alexanderson *et al.*, 2012). At present, there is been limited evidence showing improvement in vasomotor function in response to treatment. Whether or not reversal of these mild flow abnormalities has an effect on future risk is not certain. Future studies are needed.

Cardiac radionuclide imaging (SPECT and PET) cannot visualize atherosclerotic changes in the coronary arteries *per se* (Schuijf *et al.*, 2006; Di Carli *et al.*, 2007a,b). Computed tomography coronary angiography (CTA) appears superior to PET or SPECT in estimating atherosclerosis and stenosis in the coronary vessels. Hence, the latest hybrid PET/CT scanners, similar to SPECT/CT, allow a genuine integration of anatomy and physiology, which may provide improved risk stratification (van Werkhoven *et al.*, 2009). Several studies confirm the expediency of hybrid PET/CT scanners in detecting CAD and viably myocardium in chronic and new-onset heart failure, thus facilitating the determination of heart failure aetiology and guiding a therapeutic strategy (Sheikine & Di Carli, 2008). Coronary artery calcification (CAC) by CT and MPI, either by SPECT or PET, has also demonstrated complementary applications in hybrid scanners. For example, increasing CAC scores add to risk of adverse events in patients with and without ischaemia on PET MPI (Schenker *et al.*, 2008). In selected patients, hybrid imaging may aid in more accurate diagnosis, risk stratification and management in a 'single point of contact' setting (Hsiao *et al.*, 2010).

In contrast to cardiac SPECT, image acquisition starts immediately after infusion of ^{82}Rb in cardiac PET. ECG gating under pharmacological stress test can therefore reveal LVEF and wall motion in close relation to peak hyperaemia. ECG-gated studies suggest that subjects without CAD exhibit a rise in LVEF during pharmacological adenosine stress. Subjects with IHD display a rise in LVEF that is inversely correlated with the degree of coronary artery stenosis determined by coronary angiography (Dorbala *et al.*, 2007). In addition, subjects with 3-vessel or left main coronary artery (LM) disease may demonstrate a drop in LVEF under pharmacological stress test, without necessarily displaying perfusion abnormalities. This could prove to be a vital diagnostic and prognostic tool (Dorbala *et al.*, 2007).

More recently, a F-18-labelled perfusion tracer was introduced for MPI with PET (Madar *et al.*, 2006; Huisman *et al.*, 2008). Flurpiridaz, such as FDG, may be distributed to provincial hospitals, in which a cyclotron is not available. Thus, cardiac PET MPI can be performed without a cyclotron and without the costly ^{82}Sr/^{82}Rb-generator, which demands a high patient flow. However, the costs of Flurpiridaz remain unclear. The radiotracer has a high first-pass extraction fraction of 94% and is currently being evaluated in phase three clinical studies. The 110-min half-life of ^{18}F permits its distribution as a single-unit dose on a daily basis. Moreover, the longer half-life of ^{18}F allows the application of the perfusion agent during treadmill exercise, rather than with vasodilator stress alone, as is currently the case with ^{82}Rb PET myocardial perfusion studies. However, compared with ^{82}Rb, it is not possible to perform both rest and stress imaging within 30 min.

Radiation dosimetry

PET positron emission tracers usually lead to lower radiation exposure than SPECT tracers, mostly driven by shorter half-life of PET tracers. See Table 1. Effective dosages at routine examinations with PET tracers at rest and exercise myocardial perfusion tests are lower than SPECT (Thompson & Cullom, 2006). Due to differences in tracer administration and form, the radiation dose for the staff is approximately six times lower at a combined rest and stress test, compared with a 2-day protocol with ^{99m}Tc-labelled tracer (Clarke *et al.*, 1997; Schleipman *et al.*, 2006). PET is therefore superior to SPECT regarding radiation dosage (Senthamizhchelvan *et al.*, 2010).

The typical effective dose to a patient receiving 2 × 1110 MBq ^{82}Rb is 2·8 mSv, and with additional attenuation CT and calcium score CT, the total effective dose is 3·2–5·2 mSv (Senthamizhchelvan *et al.*, 2010). The total dose to staff per patient (from routine stress and rest test) is 0·6 μSv (2 × 1110 MBq ^{82}Rb) versus 3·1 μSv (2 × 700 MBq ^{99m}Tc sestamibi). However, staff members may be exposed to higher radiation doses, in both modalities, if a medical emergency requiring staff intervention occurs (Davidson *et al.*, 2011).

Table 1 Radiation dose for adults in cardiac nuclear imaging.

Radio pharmacy	Half-life	Procedure	Effective dose (μSv/MBq)	Dose, MBq	Effective dose, mSv
^{99m}Tc-sestamibi	6 h	Rest	9·0	700–900	6·3–8·1
		Stress	7·9	700–900	5·5–7·1
^{99m}Tc-tetrofosmine	6 h	Rest	7·6	700–900	5·3–6·8
		Stress	7·0	700–900	4·9–6·3
^{201}TI	73 h	Rest/Stress	220	80–130	17·6–28·6
$^{13}NH_3$	10 min	Rest/Stress	2	370–740	0·7–1·5
^{82}Rb	75 s	Rest/Stress	1·25	1100–1500	1·4–1·9
$H_2{}^{15}O$	112 s	Rest/Stress	0·93	700–1500	0·7–1·4

^{99m}Tc, technetium-99m; ^{201}TI, thallium-201; $^{13}NH_3$, ^{13}N-labelled ammonia; ^{82}Rb, rubidium-82; $H_2{}^{15}O$, ^{15}O-labelled water; μSv, microSivert; mSv, milliSvert; MBq: megabecquerel.
Rest: cardiac perfusion imaging obtained during rest. Stress: cardiac perfusion imaging obtained during pharmacological and/or exercise stress test.

Economy

PET and SPECT

At Rigshospitalet, Copenhagen University Hospital, we estimate a demand of approximately 15 examinations per week with ^{82}Rb. The costs generated (generator + infusion system + disposables) are around 400€ per patient, whereas cardiac SPECT is 230€. However, it is expected that logistical efficiency will increase and lower the costs of personnel with a 1-day protocol operating PET as opposed to 2-day protocol narrowing the difference in price between PET and SPECT further. The traditional rest/stress cardiac SPECT can also be performed in a 1-day protocol. However, the protocol is somewhat inefficient, often taking 3–5 h to complete. This limits ability to control costs (Bateman, 2012).

Another important aspect is the reimbursement generated by PET and SPECT, respectively. A study from 2007 examined downstream invasive procedure utilization of diagnostic arteriography, comparing PET to SPECT. They concluded that cardiac PET in patients with intermediate pre-test likelihood of CAD resulted in a 50% reduction in invasive coronary arteriography and coronary artery bypass grafting, a 30% cost savings, and excellent clinical outcome at 1 year compared with SPECT (Merhige *et al.*, 2007).

Conclusion

PET myocardial perfusion imaging with ^{82}Rb has a number of advantages: improved image quality, higher diagnostic accuracy, less radiation dose to patient and staff as well as rapid examinations time. With the fast propagation of combined PET/CT scanners, we anticipate an increase in PET myocardial perfusion imaging in Europe.

Conflict of interest

The authors have no conflicts of interest.

Authors contribution

All authors contributed to the review and approved the final version of the article.

References

Aarnoudse WH, Botman KJ, Pijls NH. False-negative myocardial scintigraphy in balanced three-vessel disease, revealed by coronary pressure measurement. *Int J Cardiovasc Intervent* (2003); **5**: 67–71.

Alexanderson E, Jacome R, Jimenez-Santos M, Ochoa JM, Romero E, Cabral MA, Ricalde A, Inarra F, Meave A, Alexanderson G. Evaluation of the endothelial function in hypertensive patients with 13N-ammonia PET. *J Nucl Cardiol* (2012); **19**: 979–986.

Bateman TM. Advantages and disadvantages of PET and SPECT in a busy clinical practice. *J Nucl Cardiol* (2012); **19**(Suppl 1): S3–S11.

Camici PG, Crea F. Coronary microvascular dysfunction. *N Engl J Med* (2007); **356**: 830–840.

Clarke EA, Notghi A, Harding LK. Are MIBI/tetrofosmin heart studies a potential radiation hazard to technologists? *Nucl Med Commun* (1997); **18**: 574–577.

Davidson G, Tout D, Hurley C, Bartley M, Bradley A, Tonge C, Arumugam P. Comparative evaluation of staff dose from myocardial perfusion imaging using 82Rb PET-CT and 99mTc SPECT-CT. *Eur J Nucl Med Mol Imaging* (2011); **38**(Suppl 2): 93–228.

Di Carli MF, Lipton MJ. *Cardiac Pet and PET/CT Imaging* (2007). Springer Science+Business Media LLC, New York.

Di Carli MF, Dorbala S, Curillova Z, Kwong RJ, Goldhaber SZ, Rybicki FJ, Hachamovitch R. Relationship between CT coronary angiography and stress perfusion imaging in patients with suspected ischemic heart disease assessed by integrated PET-CT imaging. *J Nucl Cardiol* (2007a); **14**: 799–809.

Di Carli MF, Dorbala S, Meserve J, El Fakhri G, Sitek A, Moore SC. Clinical myocardial perfusion PET/CT. *J Nucl Med* (2007b); **48**: 783–793.

Dorbala S, Vangala D, Sampson U, Limaye A, Kwong R, Di Carli MF. Value of vasodilator left ventricular ejection fraction reserve in evaluating the magnitude of myocardium at risk and the extent of angiographic coronary artery disease: a 82Rb PET/CT study. *J Nucl Med* (2007); **48**: 349–358.

Dorbala S, Di Carli MF, Beanlands RS, Merhige ME, Williams BA, Veledar E, Chow BJ, Min JK, Pencina MJ, Berman DS, Shaw LJ. Prognostic value of stress myocardial perfusion positron emission tomography: results from a multicenter observational registry. *J Am Coll Cardiol* (2013); **61**: 176–184.

El Fakhri G, Kardan A, Sitek A, Dorbala S, Abi-Hatem N, Lahoud Y, Fischman A, Coughlan M, Yasuda T, Di Carli MF. Reproducibility and accuracy of quantitative myocardial blood flow assessment with (82)Rb PET: comparison with (13)N-ammonia PET. *J Nucl Med* (2009); **50**: 1062–1071.

Goldstein RA, Mullani NA, Marani SK, Fisher DJ, Gould KL, O'Brien HA Jr. Myocardial perfusion with rubidium-82. II. Effects of metabolic and pharmacologic interventions. *J Nucl Med* (1983); **24**: 907–915.

Hachamovitch R, Hayes SW, Friedman JD, Cohen I, Berman DS. Stress myocardial perfusion single-photon emission computed tomography is clinically effective and cost effective in risk stratification of patients with a high likelihood of coronary artery disease (CAD) but no known CAD. *J Am Coll Cardiol* (2004); **43**: 200–208.

Herzog BA, Husmann L, Valenta I, Gaemperli O, Siegrist PT, Tay FM, Burkhard N, Wyss CA, Kaufmann PA. Long-term prognostic value of 13N-ammonia myocardial perfusion positron emission tomography added value of coronary flow reserve. *J Am Coll Cardiol* (2009); **54**: 150–156.

Hesse B, Lindhardt TB, Acampa W, Anagnostopoulos C, Ballinger J, Bax JJ, Edenbrandt L, Flotats A, Germano G, Stopar TG, Franken P, Kelion A, Kjaer A, Le Guludec D, Ljungberg M, Maenhout AF, Marcassa C, Marving J, McKiddie F, Schaefer WM, Stegger L, Underwood R. EANM/ESC guidelines for radionuclide imaging of cardiac function. *Eur J Nucl Med Mol Imaging* (2008); **35**: 851–885.

Hsiao EM, Ali B, Dorbala S. Clinical role of hybrid imaging. *Curr Cardiovasc Imaging Rep* (2010); **3**: 324–335.

Huisman MC, Higuchi T, Reder S, Nekolla SG, Poethko T, Wester HJ, Ziegler SI, Casebier DS, Robinson SP, Schwaiger M. Initial characterization of an 18F-labeled myocar-

dial perfusion tracer. *J Nucl Med* (2008); **49**: 630–636.

Ito Y, Katoh C, Noriyasu K, Kuge Y, Furuyama H, Morita K, Kohya T, Kitabatake A, Tamaki N. Estimation of myocardial blood flow and myocardial flow reserve by 99mTc-sestamibi imaging: comparison with the results of [15O]H2O PET. *Eur J Nucl Med Mol Imaging* (2003); **30**: 281–287.

Kaufmann PA, Gnecchi-Ruscone T, di Terlizzi M, Schafers KP, Luscher TF, Camici PG. Coronary heart disease in smokers: vitamin C restores coronary microcirculatory function. *Circulation* (2000); **102**: 1233–1238.

deKemp RA, Yoshinaga K, Beanlands RS. Will 3-dimensional PET-CT enable the routine quantification of myocardial blood flow? *J Nucl Cardiol* (2007); **14**: 380–397.

Kjaer A, Cortsen A, Rahbek B, Hasseldam H, Hesse B. Attenuation and scatter correction in myocardial SPET: improved diagnostic accuracy in patients with suspected coronary artery disease. *Eur J Nucl Med Mol Imaging* (2002); **29**: 1438–1442.

Kjaer A, Meyer C, Nielsen FS, Parving HH, Hesse B. Dipyridamole, cold pressor test, and demonstration of endothelial dysfunction: a PET study of myocardial perfusion in diabetes. *J Nucl Med* (2003); **44**: 19–23.

Kjaer A, Meyer C, Wachtell K, Olsen MH, Ibsen H, Opie L, Holm S, Hesse B. Positron emission tomographic evaluation of regulation of myocardial perfusion in physiological (elite athletes) and pathological (systemic hypertension) left ventricular hypertrophy. *Am J Cardiol* (2005); **96**: 1692–1698.

Klocke FJ, Baird MG, Lorell BH, Bateman TM, Messer JV, Berman DS, O'Gara PT, Carabello BA, Russell RO Jr, Cerqueira MD, St John Sutton MG, DeMaria AN, Udelson JE, Kennedy JW, Verani MS, Williams KA, Antman EM, Smith SC Jr, Alpert JS, Gregoratos G, Anderson JL, Hiratzka LF, Faxon DP, Hunt SA, Fuster V, Jacobs AK, Gibbons RJ, Russell RO. ACC/AHA/ASNC guidelines for the clinical use of cardiac radionuclide imaging–executive summary: a report of the American College of Cardiology/American Heart Association Task Force on Practice Guidelines (ACC/AHA/ASNC Committee to Revise the 1995 Guidelines for the Clinical Use of Cardiac Radionuclide Imaging). *Circulation* (2003); **108**: 1404–1418.

Kristoffersen US, Wiinberg N, Petersen CL, Gerstoft J, Gutte H, Lebech AM, Kjaer A. Reduction in coronary and peripheral vasomotor function in patients with HIV after initiation of antiretroviral therapy: a longitudinal study with positron emission tomography and flow-mediated dilation. *Nucl Med Commun* (2010); **31**: 874–880.

Kuhle WG, Porenta G, Huang SC, Buxton D, Gambhir SS, Hansen H, Phelps ME, Schelbert HR. Quantification of regional myocardial blood flow using 13N-ammonia and reoriented dynamic positron emission tomographic imaging. *Circulation* (1992); **86**: 1004–1017.

Lima RS, Watson DD, Goode AR, Siadaty MS, Ragosta M, Beller GA, Samady H. Incremental value of combined perfusion and function over perfusion alone by gated SPECT myocardial perfusion imaging for detection of severe three-vessel coronary artery disease. *J Am Coll Cardiol* (2003); **42**: 64–70.

Lin JW, Laine AF, Akinboboye O, Bergmann SR. Use of wavelet transforms in analysis of time-activity data from cardiac PET. *J Nucl Med* (2001a); **42**: 194–200.

Lin JW, Laine AF, Bergmann SR. Improving PET-based physiological quantification through methods of wavelet denoising. *IEEE Trans Biomed Eng* (2001b); **48**: 202–212.

Madar I, Ravert HT, Du Y, Hilton J, Volokh L, Dannals RF, Frost JJ, Hare JM. Characterization of uptake of the new PET imaging compound 18F-fluorobenzyl triphenyl phosphonium in dog myocardium. *J Nucl Med* (2006); **47**: 1359–1366.

Marcassa C, Bax JJ, Bengel F, Hesse B, Petersen CL, Reyes E, Underwood R. Clinical value, cost-effectiveness, and safety of myocardial perfusion scintigraphy: a position statement. *Eur Heart J* (2008); **29**: 557–563.

Mc Ardle BA, Dowsley TF, deKemp RA, Wells GA, Beanlands RS. Does rubidium-82 PET have superior accuracy to SPECT perfusion imaging for the diagnosis of obstructive coronary disease?: A systematic review and meta-analysis. *J Am Coll Cardiol* (2012); **60**: 1828–1837.

Merhige ME, Breen WJ, Shelton V, Houston T, D'Arcy BJ, Perna AF. Impact of myocardial perfusion imaging with PET and (82) Rb on downstream invasive procedure utilization, costs, and outcomes in coronary disease management. *J Nucl Med* (2007); **48**: 1069–1076.

Mullani NA, Goldstein RA, Gould KL, Marani SK, Fisher DJ, O'Brien HA Jr, Loberg MD. Myocardial perfusion with rubidium-82. I. Measurement of extraction fraction and flow with external detectors. *J Nucl Med* (1983); **24**: 898–906.

Muzik O, Beanlands RS, Hutchins GD, Mangner TJ, Nguyen N, Schwaiger M. Validation of nitrogen-13-ammonia tracer kinetic model for quantification of myocardial blood flow using PET. *J Nucl Med* (1993); **34**: 83–91.

Navare SM, Mather JF, Shaw LJ, Fowler MS, Heller GV. Comparison of risk stratification with pharmacologic and exercise stress myocardial perfusion imaging: a meta-analysis. *J Nucl Cardiol* (2004); **11**: 551–561.

Naya M, Murthy VL, Foster CR, Gaber M, Klein J, Hainer J, Dorbala S, Blankstein R, Di Carli MF. Prognostic interplay of coronary artery calcification and underlying vascular dysfunction in patients with suspected coronary artery disease. *J Am Coll Cardiol* (2013); **61**: 2098–2106.

Nitzsche EU, Choi Y, Czernin J, Hoh CK, Huang SC, Schelbert HR. Noninvasive quantification of myocardial blood flow in humans. A direct comparison of the [13N]ammonia and the [15O]water techniques. *Circulation* (1996); **93**: 2000–2006.

Parkash R, deKemp RA, Ruddy TD, Kitsikis A, Hart R, Beauchesne L, Williams K, Davies RA, Labinaz M, Beanlands RS. Potential utility of rubidium 82 PET quantification in patients with 3-vessel coronary artery disease. *J Nucl Cardiol* (2004); **11**: 440–449.

Prior JO, Allenbach G, Valenta I, Kosinski M, Burger C, Verdun FR, Bischof Delaloye A, Kaufmann PA. Quantification of myocardial blood flow with 82Rb positron emission tomography: clinical validation with 15O-water. *Eur J Nucl Med Mol Imaging* (2012); **39**: 1037–1047.

Rahmim A, Zaidi H. PET versus SPECT: strengths, limitations and challenges. *Nucl Med Commun* (2008); **29**: 193–207.

Rigo P, Van Boxem P, Foulon J, Safi M, Engdahl J, Links J. Quantitative evaluation of a comprehensive motion, resolution, and attenuation correction program: initial experience. *J Nucl Cardiol* (1998); **5**: 458–468.

Schelbert HR, Phelps ME, Hoffman EJ, Huang SC, Selin CE, Kuhl DE. Regional myocardial perfusion assessed with N-13 labeled ammonia and positron emission computerized axial tomography. *Am J Cardiol* (1979); **43**: 209–218.

Schelbert HR, Phelps ME, Huang SC, MacDonald NS, Hansen H, Selin C, Kuhl DE. N-13 ammonia as an indicator of myocardial blood flow. *Circulation* (1981); **63**: 1259–1272.

Schelbert HR, Wisenberg G, Phelps ME, Gould KL, Henze E, Hoffman EJ, Gomes A, Kuhl DE. Noninvasive assessment of coronary stenoses by myocardial imaging during pharmacologic coronary vasodilation. VI. Detection of coronary artery disease in human beings with intravenous N-13 ammonia and positron computed tomography. *Am J Cardiol* (1982); **49**: 1197–1207.

Schenker MP, Dorbala S, Hong EC, Rybicki FJ, Hachamovitch R, Kwong RY, Di Carli MF. Interrelation of coronary calcification, myocardial ischemia, and outcomes in patients with intermediate likelihood of cor-

onary artery disease: a combined positron emission tomography/computed tomography study. *Circulation* (2008); **117**: 1693–1700.

Schindler TH, Cardenas J, Prior JO, Facta AD, Kreissl MC, Zhang XL, Sayre J, Dahlbom M, Licinio J, Schelbert HR. Relationship between increasing body weight, insulin resistance, inflammation, adipocytokine leptin, and coronary circulatory function. *J Am Coll Cardiol* (2006); **47**: 1188–1195.

Schindler TH, Facta AD, Prior JO, Cadenas J, Zhang XL, Li Y, Sayre J, Goldin J, Schelbert HR. Structural alterations of the coronary arterial wall are associated with myocardial flow heterogeneity in type 2 diabetes mellitus. *Eur J Nucl Med Mol Imaging* (2009); **36**: 219–229.

Schleipman AR, Castronovo FP Jr, Di Carli MF, Dorbala S. Occupational radiation dose associated with Rb-82 myocardial perfusion positron emission tomography imaging. *J Nucl Cardiol* (2006); **13**: 378–384.

Schuijf JD, Wijns W, Jukema JW, Atsma DE, de Roos A, Lamb HJ, Stokkel MP, Dibbets-Schneider P, Decramer I, De Bondt P, van der Wall EE, Vanhoenacker PK, Bax JJ. Relationship between noninvasive coronary angiography with multi-slice computed tomography and myocardial perfusion imaging. *J Am Coll Cardiol* (2006); **48**: 2508–2514.

Selwyn AP, Allan RM, L'Abbate A, Horlock P, Camici P, Clark J, O'Brien HA, Grant PM. Relation between regional myocardial uptake of rubidium-82 and perfusion: absolute reduction of cation uptake in ischemia. *Am J Cardiol* (1982); **50**: 112–121.

Senthamizhchelvan S, Bravo PE, Esaias C, Lodge MA, Merrill J, Hobbs RF, Sgouros G, Bengel FM. Human biodistribution and radiation dosimetry of 82Rb. *J Nucl Med* (2010); **51**: 1592–1599.

Shaw LJ, Iskandrian AE. Prognostic value of gated myocardial perfusion SPECT. *J Nucl Cardiol* (2004); **11**: 171–185.

Sheikine Y, Di Carli MF. Integrated PET/CT in the assessment of etiology and viability in ischemic heart failure. *Curr Heart Fail Rep* (2008); **5**: 136–142.

Storto G, Soricelli A, Pellegrino T, Petretta M, Cuocolo A. Assessment of the arterial input function for estimation of coronary flow reserve by single photon emission computed tomography: comparison of two different approaches. *Eur J Nucl Med Mol Imaging* (2009); **36**: 2034–2041.

Tamaki N, Yonekura Y, Senda M, Yamashita K, Koide H, Saji H, Hashimoto T, Fudo T, Kambara H, Kawai C, Konishi J., *et al.* Value and limitation of stress thallium-201 single photon emission computed tomography: comparison with nitrogen-13 ammonia positron tomography. *J Nucl Med* (1988); **29**: 1181–1188.

Thompson RC, Cullom SJ. Issues regarding radiation dosage of cardiac nuclear and radiography procedures. *J Nucl Cardiol* (2006); **13**: 19–23.

Venkataraman R, Hage FG, Dorfman T, Heo J, Aqel RA, de Mattos AM, Iskandrian AE. Role of myocardial perfusion imaging in patients with end-stage renal disease undergoing coronary angiography. *Am J Cardiol* (2008); **102**: 1451–1456.

Walsh MN, Bergmann SR, Steele RL, Kenzora JL, Ter-Pogossian MM, Sobel BE, Geltman EM. Delineation of impaired regional myocardial perfusion by positron emission tomography with H2(15)O. *Circulation* (1988); **78**: 612–620.

van Werkhoven JM, Schuijf JD, Gaemperli O, Jukema JW, Boersma E, Wijns W, Stolzmann P, Alkadhi H, Valenta I, Stokkel MP, Kroft LJ, de Roos A, Pundziute G, Scholte A, van der Wall EE, Kaufmann PA, Bax JJ. Prognostic value of multislice computed tomography and gated single-photon emission computed tomography in patients with suspected coronary artery disease. *J Am Coll Cardiol* (2009); **53**: 623–632.

Wijns W, Kolh P, Danchin N, Di Mario C, Falk V, Folliguet T, Garg S, Huber K, James S, Knuuti J, Lopez-Sendon J, Marco J, Menicanti L, Ostojic M, Piepoli MF, Pirlet C, Pomar JL, Reifart N, Ribichini FL, Schalij MJ, Sergeant P, Serruys PW, Silber S, Sousa Uva M, Taggart D. Guidelines on myocardial revascularization. *Eur Heart J* (2010); **31**: 2501–2555.

Yoshida K, Mullani N, Gould KL. Coronary flow and flow reserve by PET simplified for clinical applications using rubidium-82 or nitrogen-13-ammonia. *J Nucl Med* (1996); **37**: 1701–1712.

Zaret BL, Cohen LS. Cardiovascular nuclear medicine II: evaluation of perfusion and viability. *Mod Concepts Cardiovasc Dis* (1977); **46**: 37–42.

